NASA TECHNICAL NOTE

NASA TN D-2960

NASA TN D-2960

BUCKLING OF ECCENTRICALLY STIFFENED ORTHOTROPIC CYLINDERS

by David L. Block, Michael F. Card, and Martin M. Mikulas, Jr.

Langley Research Center
Langley Station, Hampton, Va.

NATIONAL AERONAUTICS AND SPACE ADMINISTRATION • WASHINGTON, D. C. • AUGUST 1965

NASA TN D-2960

BUCKLING OF ECCENTRICALLY STIFFENED ORTHOTROPIC CYLINDERS

By David L. Block, Michael F. Card,
and Martin M. Mikulas, Jr.

Langley Research Center
Langley Station, Hampton, Va.

NATIONAL AERONAUTICS AND SPACE ADMINISTRATION

For sale by the Clearinghouse for Federal Scientific and Technical Information
Springfield, Virginia 22151 – Price $2.00

BUCKLING OF ECCENTRICALLY STIFFENED ORTHOTROPIC CYLINDERS

By David L. Block, Michael F. Card,
and Martin M. Mikulas, Jr.
Langley Research Center

SUMMARY

A small-deflection theory for buckling of stiffened orthotropic cylinders which includes eccentricity (one-sided) effects in the stiffeners is derived from energy principles. Buckling solutions corresponding to classical simple-support boundary conditions are obtained for both orthotropic and isotropic stiffened cylinders subjected to any combination of axial and circumferential loading. Comparable solutions for stiffened flat plates are also given. Sample calculations of predicted compressive buckling loads obtained from the solutions are compared with existing solutions for ring-stiffened corrugated cylinders, ring-and-stringer-stiffened cylinders, and longitudinally (stringer) stiffened cylinders. The calculations demonstrate that eccentricity effects are large even with very large diameter cylinders of practical proportions and should be accounted for in any buckling analysis.

INTRODUCTION

As early as 1947, Van der Neut (ref. 1) demonstrated the importance of eccentricity or one-sidedness of stiffening elements in determining the buckling strength of stiffened cylindrical shells. Unfortunately, this early work seems to have been largely neglected. More recent theoretical work (refs. 2, 3, and 4) indicates a renewed interest in eccentricity effects in stiffened shell structures. Recent experimental results (refs. 3, 4, and 5) have shown that the eccentricity effects suggested by theory are real and large enough to warrant their appraisal in design.

In view of the great variety of stiffened shell configurations that are now under consideration by structural designers, a buckling analysis of stiffened cylindrical shells which includes eccentricity effects and is applicable to a broad class of structures is needed. A buckling analysis that has a wide range of applicability can be obtained by considering a cylindrical shell constructed from an orthotropic material having stiffening elements on its surface. With appropriate definitions of the orthotropic material constants, such an analysis can be used to predict buckling for a wide variety of stiffened shells, for example sandwich-type, corrugated, or filament-wound cylinders.

The purpose of the present paper is to present a small deflection theory for buckling of an orthotropic cylinder stiffened by both stringers and rings. The theory includes stiffener eccentricity effects and represents a generalization of the work by Baruch and Singer (ref. 2) for ring-and-stringer-stiffened isotropic shells. The theory is a classical buckling theory in that the effect of prebuckling deformations is neglected and only small deflections are considered. The buckling equations and boundary conditions are derived in a consistent manner from the potential energy of the loaded stiffened shell. Solutions to the equations corresponding to boundary conditions analogous to classical simple support in isotropic shell theory are obtained for cylinders subjected to any combination of axial and circumferential loading. Sample calculations of predicted compressive buckling loads obtained from the solutions are compared with existing solutions for ring-stiffened corrugated cylinders, for ring-and-stringer-stiffened cylinders, and for longitudinally stiffened cylinders.

SYMBOLS

The units used for the physical quantities in this report are given both in the U.S. Customary Units and in the International System of Units, SI. The relationship between these two systems of units can be found in reference 6.

A	cross-sectional area of stiffener
D	bending stiffness of isotropic plate, $\frac{Et^3}{12(1-\mu^2)}$
D_x, D_y	bending stiffnesses of orthotropic plate in longitudinal and circumferential directions, respectively
D_{xy}	twisting stiffness of orthotropic plate
E	Young's modulus
E_x, E_y	extensional stiffnesses of orthotropic plate in longitudinal and circumferential directions, respectively
G	shear modulus
G_{xy}	in-plane shear stiffness of orthotropic plate
I	moment of inertia of stiffener about its centroid
I_o	moment of inertia of stiffener about middle surface of shell
J	torsional constant for stiffener

M_x, M_y, M_{xy} bending and twisting moments in orthotropic shell

N_x, N_y, N_{xy} normal and shearing forces in orthotropic shell

$\bar{N}_x, \bar{N}_y, \bar{N}_{xy}$ applied compressive and shear loads

R radius of cylinder to middle surface of orthotropic shell (see fig. 1)

$\bar{R}$ extensional stiffness ratio for ring, $\frac{E_r A_r}{Et\ell}$

$\bar{S}$ extensional stiffness ratio for stringer, $\frac{E_s A_s}{Etd}$

Z curvature parameter, $\frac{a^2\sqrt{(1 - \mu^2)}}{Rt}$

a length of stiffened cylinder (see fig. 1)

d stringer spacing (see fig. 1)

ℓ ring spacing (see fig. 1)

m number of half waves in the cylinder buckle pattern in longitudinal direction

n number of full waves in the cylinder buckle pattern in circumferential direction

p width of element of corrugation (see fig. 2)

t thickness of cylinder shell wall (see fig. 1)

$\bar{t}$ effective wall thickness of stiffened isotropic cylinder, $\frac{A_s}{d} + t$

t_c thickness of corrugation (see fig. 2)

u, v, w displacements in x-, y-, and z-directions, respectively, of a point in middle surface of orthotropic shell

$\bar{u}, \bar{v}, \bar{w}$ amplitudes of buckling displacements

x, y, z orthogonal curvilinear coordinates with origin lying in middle surface of orthotropic shell (see fig. 1)

$\bar{z}$ distance from centroid of stiffener to middle surface of orthotropic shell (see fig. 1), positive if stiffener lies on external surface of shell

$\alpha = \frac{m\pi R}{a}$

$\beta = \frac{na}{m\pi R}$

Π total change in potential energy of loaded stiffened cylinder

Π_c, Π_r, Π_s change in strain energy of orthotropic shell, rings, and stringers, respectively

Π_L change in potential energy of external forces

$\epsilon_x, \epsilon_y, \gamma_{xy}$ strains at middle surface of orthotropic shell

$\epsilon_{x_T}, \epsilon_{y_T}, \gamma_{xy_T}$ strains in orthotropic shell

$\epsilon_{x_s}, \epsilon_{y_r}$ strains in stringers and rings, respectively

θ corrugation angle (see fig. 2)

Λ defined by equation (17)

μ Poisson's ratio

μ_x, μ_y Poisson's ratios for bending of orthotropic plate in longitudinal and circumferential directions, respectively

μ_x', μ_y' Poisson's ratios for extension of orthotropic plate in longitudinal and circumferential directions, respectively

Subscripts:

s,r denote properties of stringers (longitudinal stiffening, parallel to x-axis) and rings (transverse stiffening, parallel to y-axis), respectively

x,y longitudinal and circumferential directions, respectively

A subscript preceded by a comma denotes partial differentiation with respect to the subscript.

DERIVATION OF THEORY

In developing the theory for the stiffened cylinder shown in figure 1, several basic assumptions are made. The stiffened cylinder is considered to be

composed of an orthotropic shell stiffened by uniform equally spaced stringers and rings, all having elastic material properties. The elastic constants of the orthotropic shell are taken as those given in reference 7. However, for the present analysis the transverse shearing stiffnesses of the shell are assumed to be infinitely large. The rings and stringers are assumed to be spaced closely so that their elastic properties can be averaged over the stiffener spacing. The usual Donnell-type assumptions are used to specify buckling displacements in the shell, whereas the stiffeners are treated as beam elements with stiffener twisting accounted for in an approximate manner. In cases where both rings and stringers lie on the same surface of the shell, the effect of joints in the stiffener framework is ignored.

The theory is derived by obtaining strain energy expressions corresponding to buckling displacements in the shell and stiffeners and by applying the method of minimum potential energy to obtain the equilibrium equations of the system. The following sections detail the derivation of the strain energy for the orthotropic shell and stiffeners, and present the corresponding equilibrium equations governing the buckling behavior of the stiffened cylinder.

Strain-Displacement Relations

For the coordinate system shown in figure 1, the strain-displacement relations in the orthotropic shell due to buckling displacements can be written as

$$\left.\begin{aligned} \epsilon_{x_T} &= \epsilon_x - zw_{,xx} \\ \epsilon_{y_T} &= \epsilon_y - zw_{,yy} \\ \gamma_{xy_T} &= \gamma_{xy} - 2zw_{,xy} \end{aligned}\right\} \qquad (1)$$

with

$$\epsilon_x = u_{,x}$$

$$\epsilon_y = v_{,y} + \frac{w}{R}$$

$$\gamma_{xy} = u_{,y} + v_{,x}$$

Equations (1) are the usual strain-displacement relations of Donnell-type shell buckling theory where u, v, and w are the additional displacements induced by buckling.

If the stiffeners are assumed to behave as beam elements, the stiffener strain-displacement relations can be written as

$$\left.\begin{aligned} \epsilon_{x_s} &= \epsilon_x - zw,_{xx} \\ \epsilon_{y_r} &= \epsilon_y - zw,_{yy} \end{aligned}\right\} \tag{2}$$

where the subscripts s and r are used to denote stringers and rings, respectively. Equations (2) specify that buckling displacements are such that strain varies linearly across the depth of the stiffener, yet satisfies compatibility of displacements between the stiffener and the surface of the shell to which it is fastened. This compatibility requirement is the source of the eccentricity or one-sided effects in buckling of stiffened shells.

Strain Energy of the Orthotropic Shell

The change in strain energy of the orthotropic shell Π_c can be expressed in terms of resultant middle-surface forces and moments as follows:

$$\Pi_c = \frac{1}{2}\int_0^{2\pi R}\int_0^a \left(N_x\epsilon_x + N_{xy}\gamma_{xy} + N_y\epsilon_y - M_x w,_{xx} + 2M_{xy}w,_{xy} - M_y w,_{yy}\right)dx\,dy \tag{3}$$

Middle-surface force-strain relations and moment-curvature relations that are consistent with the strain-displacement relations of equations (1) are given in reference 7 as

$$\left.\begin{aligned} N_x &= \frac{E_x}{1 - \mu_x'\mu_y'}\left(\epsilon_x + \mu_y'\epsilon_y\right) \\ N_y &= \frac{E_y}{1 - \mu_x'\mu_y'}\left(\epsilon_y + \mu_x'\epsilon_x\right) \\ N_{xy} &= G_{xy}\gamma_{xy} \\ M_x &= -\frac{D_x}{1 - \mu_x\mu_y}\left(w,_{xx} + \mu_y w,_{yy}\right) \\ M_y &= -\frac{D_y}{1 - \mu_x\mu_y}\left(w,_{yy} + \mu_x w,_{xx}\right) \\ M_{xy} &= D_{xy}w,_{xy} \end{aligned}\right\} \tag{4}$$

Substituting equations (4) into equation (3) and using equations (1) yields the following strain energy expression for the orthotropic shell

$$\Pi_c = \frac{1}{2}\int_0^{2\pi R}\int_0^a \left[\frac{E_x}{1-\mu_x'\mu_y'}u_{,x}^2 + \frac{\mu_y'E_x + \mu_x'E_y}{1-\mu_x'\mu_y'}u_{,x}\left(v_{,y}+\frac{w}{R}\right)\right.$$

$$+ G_{xy}\left(v_{,x}+u_{,y}\right)^2 + \frac{E_y}{1-\mu_x'\mu_y'}\left(v_{,y}+\frac{w}{R}\right)^2 + \frac{D_x}{1-\mu_x\mu_y}w_{,xx}^2$$

$$\left. + \frac{\mu_y D_x + \mu_x D_y}{1-\mu_x\mu_y}w_{,xx}w_{,yy} + 2D_{xy}w_{,xy}^2 + \frac{D_y}{1-\mu_x\mu_y}w_{,yy}^2\right]dx\,dy \qquad (5)$$

Strain Energy of Stiffeners

The change in strain energy of stiffeners corresponding to buckling displacements in the stringers Π_s is taken as

$$\Pi_s = \frac{1}{2}\int_0^{2\pi R}\int_0^a \left(\int_{A_s}\frac{E_s\epsilon_{x_s}^2}{d}dA_s + \frac{G_sJ_s}{d}w_{,xy}^2\right)dx\,dy \qquad (6)$$

where dA_s denotes an element of the cross-sectional area of the stringer A_s, G_sJ_s is the twisting stiffness of the stringer section, and d is the stringer spacing.

The first term in the energy expression is the usual expression for energy associated with bending and extension of a beam. The second term has been inserted as an approximation to the energy stored as a result of twisting the stringers. (See, as an example, ref. 8.) This term is a result of assuming that the stringer twists in a fashion so that its angle of twist is equal to the angle of twist of the shell. The use of more accurate energy expressions for twisting in equation (6) complicates the solution of the buckling problem. Such expressions introduce effects which are assumed to be of little consequence in buckling of stiffened cylinders having contemporary aircraft or spacecraft proportions. The energy contributions of the stringers in equation (6) are averaged over the cylinder circumference; hence, discreteness of the stringers is ignored.

When the stringer strain-displacement relation (eqs. (2)) is substituted into equation (6) and integration over the stringer area is performed, the strain energy expression for the stringers becomes

$$\Pi_s = \frac{1}{2d} \int_0^{2\pi R} \int_0^a \left(E_s A_s u,_x^2 - 2\bar{z}_s E_s A_s u,_x w,_{xx} + E_s I_{o_s} w,_{xx}^2 + G_s J_s w,_{xy}^2 \right) dx\, dy \tag{7}$$

where $\bar{z}_s$ is the distance from the centroid of a stringer to the middle surface of the shell (see fig. 1) and is positive if the stringer is on the external surface of the cylinder, and where I_{o_s} is the moment of inertia of a stringer about the middle surface of the shell.

For the rings, the change in strain energy Π_r can be shown to be

$$\Pi_r = \frac{1}{2l} \int_0^{2\pi R} \int_0^a \left[E_r A_r \left(v,_y + \frac{w}{R} \right)^2 - 2\bar{z}_r E_r A_r \left(v,_y + \frac{w}{R} \right) w,_{yy} \right.$$

$$\left. + E_r I_{o_r} w,_{yy}^2 + G_r J_r w,_{xy}^2 \right] dx\, dy \tag{8}$$

where l is the ring spacing and the subscript r is used to denote ring properties comparable to those appearing in equation (7) for the stringers.

Potential Energy of External Forces

A rigorous derivation of the buckling equations from the potential energy of the loaded shell requires use of nonlinear theory and techniques such as those employed in reference 9. However, when the effects of prebuckling deformations are not considered explicitly as is done in the present theory, the correct loading terms in the equilibrium equations and associated boundary conditions can be obtained by use of the following expression for the change in potential energy of the forces causing buckling:

$$\Pi_L = -\frac{1}{2} \int_0^{2\pi R} \int_0^a \left(\bar{N}_x w,_x^2 + 2\bar{N}_{xy} w,_x w,_y + \bar{N}_y w,_y^2 \right) dx\, dy \tag{9}$$

In equation (9), $\bar{N}_x$ is a stress resultant (positive in compression) obtained by considering the shell and stringers to be loaded with a uniform normal stress in the x-direction. Similarly, $\bar{N}_y$ is a stress resultant (positive in compression) obtained by considering the shell and rings to be loaded with a uniform normal stress in the y-direction. For example, if the shell is loaded with an external hydrostatic pressure q, then $\bar{N}_y = qR$ and $\bar{N}_x = \frac{qR}{2}$.

Equilibrium Equations

The total change in potential energy of the loaded stiffened cylinder Π can be written as

$$\Pi = \Pi_c + \Pi_s + \Pi_r + \Pi_L \tag{10}$$

The application of the method of minimum potential energy so that $\delta\Pi = 0$ yields the following equilibrium equations corresponding to arbitrary variations in u, v, and w, respectively:

$$\frac{E_x}{1 - \mu_x'\mu_y'} u_{,xx} + \frac{E_s A_s}{d}\left(u_{,xx} - \bar{z}_s w_{,xxx}\right)$$

$$+ \frac{\mu_y' E_x}{1 - \mu_x'\mu_y'}\left(v_{,xy} + \frac{w_{,x}}{R}\right) + G_{xy}\left(u_{,yy} + v_{,xy}\right) = 0 \tag{11a}$$

$$\frac{E_y}{1 - \mu_x'\mu_y'}\left(v_{,yy} + \frac{w_{,y}}{R}\right) + \frac{E_r A_r}{l}\left(v_{,yy} + \frac{w_{,y}}{R} - \bar{z}_r w_{,yyy}\right)$$

$$+ \frac{\mu_x' E_y}{1 - \mu_x'\mu_y'} u_{,xy} + G_{xy}\left(u_{,xy} + v_{,xx}\right) = 0 \tag{11b}$$

$$\left(\frac{D_x}{1 - \mu_x\mu_y} + \frac{E_s I_{o_s}}{d}\right) w_{,xxxx} + \left(\frac{\mu_y D_x}{1 - \mu_x\mu_y} + 2D_{xy} + \frac{\mu_x D_y}{1 - \mu_x\mu_y} + \frac{G_s J_s}{d} + \frac{G_r J_r}{l}\right) w_{,xxyy}$$

$$+ \left(\frac{D_y}{1 - \mu_x\mu_y} + \frac{E_r I_{o_r}}{l}\right) w_{,yyyy} + \frac{E_y}{R\left(1 - \mu_x'\mu_y'\right)}\left(\mu_x' u_{,x} + v_{,y} + \frac{w}{R}\right)$$

$$- \frac{E_s A_s}{d} \bar{z}_s u_{,xxx} - \frac{E_r A_r}{l} \bar{z}_r\left(\frac{2w_{,yy}}{R} + v_{,yyy}\right) + \frac{E_r A_r}{Rl}\left(v_{,y} + \frac{w}{R}\right)$$

$$+ \bar{N}_x w_{,xx} + 2\bar{N}_{xy} w_{,xy} + \bar{N}_y w_{,yy} = 0 \tag{11c}$$

Equations (11) can be shown to reduce to the equilibrium equations obtained by Baruch and Singer for stiffened isotropic shells (ref. 2) if the orthotropic

constants appearing in the equation are replaced by their equivalent isotropic values, that is, if

$$\left.\begin{aligned} &\mu_x = \mu_y = \mu_x' = \mu_y' = \mu \\ &D_x = D_y = \frac{Et^3}{12} \\ &D_{xy} = \frac{Gt^3}{6} \\ &E_x = E_y = Et \\ &G_{xy} = Gt \end{aligned}\right\} \tag{12}$$

Boundary Conditions

In addition to the equilibrium equations, the variation of the potential energy yields a set of admissible boundary conditions consistent with the energy expressions employed. The resultant homogeneous boundary conditions prescribed at each end of the cylinder at the middle surface of the orthotropic shell are as follows:

$$\left.\begin{aligned} &\frac{D_x}{1-\mu_x\mu_y}\left(w_{,xx} + \mu_y w_{,yy}\right)_{,x} + \left(2D_{xy} + \frac{G_sJ_s}{d} + \frac{G_rJ_r}{l}\right)w_{,xyy} \\ &+ \frac{E_sI_{o_s}}{d}\, w_{,xxx} - \frac{E_sA_s}{d}\,\bar{z}_s u_{,xx} + \bar{N}_x w_{,x} + \bar{N}_{xy} w_{,y} = 0 \\ &\text{or} \quad w = 0 \end{aligned}\right\} \tag{13a}$$

$$\left.\begin{aligned} &\frac{D_x}{1-\mu_x\mu_y}\left(w_{,xx} + \mu_y w_{,yy}\right) + \frac{E_sI_{o_s}}{d}\, w_{,xx} - \frac{E_sA_s}{d}\,\bar{z}_s u_{,x} = 0 \\ &\text{or} \quad w_{,x} = 0 \end{aligned}\right\} \tag{13b}$$

$$\left.\begin{aligned} &\frac{E_x}{1 - \mu_x'\mu_y'}\left[u_{,x} + \mu_y'\left(v_{,y} + \frac{w}{R}\right)\right] + \frac{E_sA_s}{d}u_{,x} - \frac{E_sA_s}{d}\bar{z}_s w_{,xx} = 0 \\ &\text{or} \quad u = 0 \end{aligned}\right\} \tag{13c}$$

$$\left.\begin{aligned} &G_{xy}\left(u_{,y} + v_{,x}\right) = 0 \\ &\text{or} \quad v = 0 \end{aligned}\right\} \tag{13d}$$

The natural boundary conditions are the first conditions given in each of equations (13) and can be explained as follows: Equations (13a) require a quantity comparable to the so-called Kirchhoff shear term to be set equal to zero and hence is a free-edge boundary condition. The remaining three natural boundary conditions in equations (13b), (13c), and (13d) correspond to conditions in which the edge moment resultant, the extensional stress resultant, and the shearing stress resultant, respectively, are set equal to zero. The geometric boundary conditions are the usual conditions for displacements prescribed in isotropic cylinder theory.

SOLUTIONS TO THE EQUILIBRIUM EQUATIONS

When the stiffened cylinder is loaded with any combination of axial and circumferential loading $\left(\bar{N}_{xy} = 0\right)$, an appropriate set of displacement functions can be found which satisfy the geometric boundary conditions of equations (13a) and (13d) and the natural boundary conditions of equations (13b) and (13c). These functions are

$$\left.\begin{aligned} u &= \bar{u}\cos\frac{m\pi x}{a}\cos\frac{ny}{R} \\ v &= \bar{v}\sin\frac{m\pi x}{a}\sin\frac{ny}{R} \\ w &= \bar{w}\sin\frac{m\pi x}{a}\cos\frac{ny}{R} \end{aligned}\right\} \tag{14}$$

where m denotes the number of longitudinal half waves in the buckle pattern and n, the number of circumferential full waves. The boundary conditions

satisfied are analogous to the conditions of simple support in classical cylinder buckling theory, that is, $w = M_x = N_x = v = 0$.

Buckling of Stiffened Orthotropic Cylinders

If equations (14) are substituted into equations (11) with $\bar{N}_{xy} = 0$, the existence of nontrivial buckling displacements requires that the determinant of coefficients of $\bar{u}$, $\bar{v}$, and $\bar{w}$ vanish. This condition reduces to the stability equation

$$\left(\frac{m\pi}{a}\right)^2 \bar{N}_x + \left(\frac{n}{R}\right)^2 \bar{N}_y = A_{33} + \left(\frac{A_{12}A_{23} - A_{13}A_{22}}{A_{11}A_{22} - A_{12}^2}\right)A_{13} + \left(\frac{A_{12}A_{13} - A_{11}A_{23}}{A_{11}A_{22} - A_{12}^2}\right)A_{23} \tag{15}$$

in which

$$A_{11} = \left(\frac{E_x}{1 - \mu_x'\mu_y'} + \frac{E_sA_s}{d}\right)\left(\frac{m\pi}{a}\right)^2 + G_{xy}\left(\frac{n}{R}\right)^2$$

$$A_{12} = \left(\frac{\mu_y'E_x}{1 - \mu_x'\mu_y'} + G_{xy}\right)\left(\frac{m\pi}{a}\right)\left(\frac{n}{R}\right)$$

$$A_{13} = \frac{1}{R}\left(\frac{\mu_y'E_x}{1 - \mu_x'\mu_y'}\right)\left(\frac{m\pi}{a}\right) + \frac{E_sA_s}{d}\bar{z}_s\left(\frac{m\pi}{a}\right)^3$$

$$A_{22} = G_{xy}\left(\frac{m\pi}{a}\right)^2 + \left(\frac{E_y}{1 - \mu_x'\mu_y'} + \frac{E_rA_r}{l}\right)\left(\frac{n}{R}\right)^2$$

$$A_{23} = \frac{1}{R}\left(\frac{E_y}{1 - \mu_x'\mu_y'} + \frac{E_rA_r}{l}\right)\left(\frac{n}{R}\right) + \frac{E_rA_r}{l}\bar{z}_r\left(\frac{n}{R}\right)^3$$

$$A_{33} = \left(\frac{D_x}{1 - \mu_x\mu_y} + \frac{E_sI_{o_s}}{d}\right)\left(\frac{m\pi}{a}\right)^4 + \left(\frac{2\mu_yD_x}{1 - \mu_x\mu_y} + 2D_{xy} + \frac{G_sJ_s}{d} + \frac{G_rJ_r}{l}\right)\left(\frac{m\pi}{a}\right)^2\left(\frac{n}{R}\right)^2$$
$$+ \left(\frac{D_y}{1 - \mu_x\mu_y} + \frac{E_rI_{o_r}}{l}\right)\left(\frac{n}{R}\right)^4 + \frac{1}{R^2}\left(\frac{E_y}{1 - \mu_x'\mu_y'} + \frac{E_rA_r}{l}\right) + 2\frac{E_rA_r}{l}\bar{z}_r\frac{n^2}{R^3}$$

where the reciprocal relations $\mu_x'E_y = \mu_y'E_x$ and $\mu_x D_y = \mu_y D_x$ have been employed to simplify the equation.

Equation (15) can be used to determine buckling loads for any specified combination of axial and circumferential loading; thus, the equation can be used to investigate buckling under axial compression or under hydrostatic or lateral pressure, or to investigate interactions between axial compression and lateral pressure. To compute buckling loads from equation (15), the specified loading must be minimized numerically for integral values of both m, the number of axial half waves in the buckle pattern, and n, the number of circumferential full waves in the buckle pattern.

A stability equation valid for compressive buckling of an unstiffened orthotropic cylinder can be obtained from equation (15) by setting $\bar{N}_y$ and the quantities with subscript r or s equal to zero. The resulting equation

$$\bar{N}_x = \left(\frac{m\pi}{a}\right)^2\left[\frac{D_x}{1-\mu_x\mu_y} + \left(\frac{2\mu_y D_x}{1-\mu_x\mu_y} + 2D_{xy}\right)\left(\frac{na}{m\pi R}\right)^2 + \frac{D_y}{1-\mu_x\mu_y}\left(\frac{na}{m\pi R}\right)^4\right] + \frac{E_x E_y}{\left(\frac{m\pi}{a}\right)^2 R^2\left[E_x - \left(2\mu_y'E_x - \frac{E_x E_y}{G_{xy}}\right)\left(\frac{na}{m\pi R}\right)^2 + E_y\left(\frac{na}{m\pi R}\right)^4\right]} \tag{16}$$

is identical to that obtained by Stein and Mayers (ref. 10, eq. (A4)) when the transverse shearing stiffnesses of the referenced equation are taken to be infinitely large. Equation (16) or forms comparable to it have been used in many contemporary compressive buckling analyses of stiffened isotropic cylinders. In such analyses, effective orthotropic constants are defined to approximate the total bending and extensional stiffnesses of the composite wall composed of shell and stiffeners. Such approximations neglect eccentricity effects and will be shown later to have serious shortcomings for compressive buckling predictions even in large diameter stiffened cylinders.

Buckling of Stiffened Isotropic Cylinders

A buckling equation for stiffened isotropic cylinders subjected to combinations of axial and circumferential loading can be obtained by substituting the isotropic relations (eqs. (12)) into equation (15). The resulting equation after some manipulation can be written as

$$\left(\bar{N}_x + \bar{N}_y\beta^2\right)\frac{a^2}{\pi^2 D} = m^2\left(1+\beta^2\right)^2 + m^2\frac{E_s I_s}{dD} + m^2\beta^4\frac{E_r I_r}{lD} + \left(\frac{G_s J_s}{dD} + \frac{G_r J_r}{lD}\right)m^2\beta^2 + \frac{12Z^2}{m^2\pi^4}\left(\frac{1 + \bar{S}\Lambda_s + \bar{R}\Lambda_r + \bar{S}\bar{R}\Lambda_{rs}}{\Lambda}\right) \tag{17}$$

where

$$\Lambda_r = 1 + 2\alpha^2\beta^2\left(1 - \beta^2\mu\right)\frac{\bar{z}_r}{R} + \alpha^4\beta^4\left(1 + \beta^2\right)^2\left(\frac{\bar{z}_r}{R}\right)^2$$

$$\Lambda_s = 1 + 2\alpha^2\left(\beta^2 - \mu\right)\frac{\bar{z}_s}{R} + \alpha^4\left(1 + \beta^2\right)^2\left(\frac{\bar{z}_s}{R}\right)^2$$

$$\Lambda_{rs} = 1 - \mu^2 + 2\alpha^2\beta^2\left(1 - \mu^2\right)\left(\frac{\bar{z}_r}{R} + \frac{\bar{z}_s}{R}\right) + \alpha^4\beta^4\left[1 - \mu^2 + 2\beta^2(1 + \mu)\right]\left(\frac{\bar{z}_r}{R}\right)^2$$

$$+ 2\alpha^4\beta^4(1 + \mu)^2\,\frac{\bar{z}_r\bar{z}_s}{R^2} + \alpha^4\beta^2\left[2(1 + \mu) + \beta^2\left(1 - \mu^2\right)\right]\left(\frac{\bar{z}_s}{R}\right)^2$$

$$\Lambda = \left(1 + \beta^2\right)^2 + 2\beta^2(1 + \mu)\left(\bar{R} + \bar{S}\right) + \left(1 - \mu^2\right)\left[\bar{S} + 2\beta^2\bar{R}\bar{S}(1 + \mu) + \beta^4\bar{R}\right]$$

with

$$Z^2 = \frac{a^4\left(1 - \mu^2\right)}{R^2t^2} \qquad D = \frac{Et^3}{12\left(1 - \mu^2\right)}$$

$$\bar{S} = \frac{E_sA_s}{Etd} \qquad \bar{R} = \frac{E_rA_r}{Et\ell}$$

$$\alpha = \frac{m\pi R}{a} \qquad \beta = \frac{na}{m\pi R}$$

Note in equation (17) that I_s and I_r are the moments of inertia of a stringer and ring, respectively, about their centroids. As in the case of equation (15), the specified combination of axial and circumferential loading must be minimized numerically for integral values of m and n in order to compute buckling loads. When the applied loadings $\bar{N}_x$ and $\bar{N}_y$ are related in the manner appropriate for external hydrostatic pressure loading, equation (17) can be shown to be identical to the result obtained by Baruch and Singer (ref. 2).

In equation (17), the effect of locating the stiffeners on the internal or external surface of the cylinder shell is reflected in the quantities Λ_r, Λ_s, and Λ_{rs} by the terms linear in $\bar{z}_r$ or $\bar{z}_s$. (The eccentricities $\bar{z}_r$ and $\bar{z}_s$ are positive when the stiffeners are located on the external surface of the cylinder and negative when the stiffeners are on the internal surface.) Note

in equation (17) that these terms are weighted by functions of m and n and that sign changes can occur in these terms depending on the buckle mode shape. This fact suggests that some caution should be exercised in predicting whether external or internal stiffening of a specified cylinder will be more effective under a given loading condition.

To illustrate the latter comment, equation (17) can be specialized to a stability equation for compressive buckling of a longitudinally stiffened cylinder by setting $\bar{N}_y$, I_r, J_r, and $\bar{R}$ all equal to zero. The resulting equation is

$$\frac{\bar{N}_x a^2}{\pi^2 D} = m^2\left(1 + \beta^2\right)^2 + m^2 \frac{E_s I_s}{dD} + m^2\beta^2 \frac{G_s J_s}{dD} + \frac{12Z^2}{m^2\pi^4}\left[\frac{1 + \bar{S}\Lambda_s}{\left(1 + \beta^2\right)^2 + 2\bar{S}\beta^2(1 + \mu) + \bar{S}\left(1 - \mu^2\right)}\right] \tag{18}$$

Equation (18) is similar to that obtained by Hedgepeth and Hall (ref. 4, eq. (12)) and differs only in that the reference equation was derived by treating the cylinder shell as a membrane and by neglecting the torsional stiffness of the stiffeners so that the first and third terms on the right-hand side of equation (18) do not appear in the reference equation.

Calculations using equation (18) reveal that longitudinally stiffened cylinders usually buckle asymmetrically ($n \neq 0$), and that cylinders which buckle in this mode and are stiffened externally may carry loads substantially greater than their internally stiffened counterparts. In fact, it has been shown experimentally that an externally stiffened cylinder can carry over twice the load sustained by its internally stiffened counterpart (ref. 5). However, in a few instances, calculations for short stiffened cylinders indicate axisymmetrical buckling ($n = 0$) for both internally and externally stiffened cylinders. For this buckle mode shape, the sign of the $\bar{z}_s$ term in Λ_s in equation (18) changes from positive to negative with the result that the magnitude of the buckling load for a cylinder with internal stiffening is slightly larger than that of its externally stiffened counterpart. Thus, for longitudinally stiffened cylinders loaded in compression, externally stiffened cylinder designs are not necessarily always superior to similar designs with internal stiffening.

Examination of equations (17) and (18) suggests that eccentricity effects are not restricted to stiffened shells, but are also present in stiffened plates. A description of the effects of eccentricity in stiffened plates can be found in the appendix.

DISCUSSION OF COMPUTED RESULTS

Generalized nondimensional buckling coefficients corresponding to minimizations of the load parameters appearing in equations (15) and (17) are impractical to present in view of the number of geometric parameters involved. However, it would seem pertinent to present some computed results for cylinders of contemporary proportions to study the magnitude of eccentricity effects as well as to compare buckling predictions of existing theories with those derived from the present paper. Accordingly, computations of compressive buckling loads were made for three types of stiffened cylinders appropriate for large diameter booster interstage structures: ring-stiffened corrugated cylinders, ring-and-stringer-stiffened isotropic cylinders, and longitudinally (stringer) stiffened isotropic cylinders. The material in the cylindrical shells and in the stiffeners was taken to be identical and a value of 0.32 was assigned to Poisson's ratio for the stiffened isotropic shells. The dimensions of the cylinders are given in figure 2.

The corrugated and ring-and-stringer-stiffened cylinders are susceptible to general instability, that is, buckling in a mode in which the rings deform radially. The ring spacings l of these cylinders were varied; the corresponding nondimensional general instability buckling loads $\bar{N}_x/E_x$ or $\bar{N}_x/E\bar{t}$ $\left(\text{where } \bar{t} \text{ is the effective thickness of the cylinder wall, } \frac{A_s}{d} + t\right)$ were computed. For large ring spacings, the ring-and-stringer-stiffened cylinders are susceptible to panel instability, that is, buckling in a mode shape in which the rings have no radial deformation. Panel instability buckling loads were computed for the ring-and-stringer-stiffened cylinders by considering the stiffened cylinder between rings to be a simply supported longitudinally stiffened cylinder having a length a equal to l. The panel instability calculations then constituted the computed results for longitudinally stiffened isotropic cylinders. Eccentricity effects in each of the three classes of stiffened cylinders were studied by moving stiffeners from the internal to the external surface of the shell.

The results of the computations are presented in table I, and in figures 3, 4, and 5. All the computations presented were performed on a digital computer by minimizing numerically the compressive buckling load for integral values of m and n. The details of the individual calculations as well as discussion of the computed results follows.

Ring-Stiffened Corrugated Cylinders

General instability predictions for the corrugated cylinders are shown in figure 3. The compressive load at buckling $\bar{N}_x/E_x$ has been plotted against the nondimensionalized ring spacing l/R. Curves are shown for the cylinders stiffened internally or externally. The solid curves in the figure were computed by employing equation (15) with $\bar{N}_y$ equal to zero and with the following values assigned to the orthotropic constants appearing in equation (15):

$$
\left.
\begin{aligned}
&\mu_x = \mu_y = \mu_x' = \mu_y' = 0 \\
&D_x = \frac{Et_c p^2}{3}\left(\frac{\sin^2\theta}{1 + \cos\theta}\right) \\
&D_{xy} = D_y = 0 \\
&E_x = 2E\left(\frac{t_c}{1 + \cos\theta}\right) \\
&G_{xy} = Gt_c\left(\frac{Et_c}{E_x}\right) \\
&E_y = 0
\end{aligned}
\right\} \qquad (19)
$$

where θ is the angle shown in figure 2, t_c is the thickness of the corrugation, and p is the width of an element of the corrugation.

The computed results indicate that eccentricity effects are quite large even though the cylinders have diameters of over 30 feet (9.2 m). Cylinders with internal rings buckle at loads that are only a third of those of the comparable externally stiffened cylinders. The result can be explained by noting that the large depth of the ring coupled with the depth of the corrugation induces very large values for the eccentricity of the rings $\bar{z}_r$. Note also that the large eccentricity produces an unusual change in buckle mode shape (see table I(a)).

The dashed curve shown in figure 3 was computed by using the Stein and Mayers buckling equation (eq. (16)). To use the equation to predict buckling of a stiffened shell, the bending and extensional stiffnesses of the stiffener-shell combination were approximated by

$$D_y = \frac{EI_r}{l}$$

$$E_y = \frac{EA_r}{l}$$

The remainder of the stiffnesses appearing in equation (16) were computed from the expressions given in equation (19).

The computation with the Stein and Mayers equation neglects the effect of eccentricity and hence represents buckling predictions for both internally and externally stiffened cylinders. Figure 3 indicates that large differences

exist between such computations and those derived from the present theory. If, however, the corrugated cylinders were symmetrically stiffened, equation (16) with the orthotropic constants just given would be expected to be a valid approximation; thus, the Stein and Mayers predictions are bracketed by predictions for cylinders with internal and external eccentricity.

Ring-and-Stringer-Stiffened Cylinders

General instability predictions for compressed ring-and-stringer-stiffened cylinders derived from equation (17) with $\bar{N}_y = 0$ are shown as the solid curves in figure 4. Three types of stringer-ring locations are shown. The differences between internal and external stiffening are not quite as large as those found for the corrugated cylinders but are nevertheless substantial with external rings and stringers appearing as the most effective stiffening configuration.

The dashed curve in figure 4 represents results computed by using the Stein and Mayers equation (eq. (16)) with the following values assigned to the orthotropic constants:

$$\mu_x = \mu_y = \mu_x' = \mu_y' = 0$$

$$D_x = \frac{E_s I_s}{d}\left[1 + \frac{\left(\bar{z}_s/\rho_s\right)^2}{1 + \frac{A_s}{dt}}\right]$$

$$D_{xy} = \frac{G}{2}\left(\frac{J_s}{d} + \frac{J_r}{l} + \frac{t^3}{3}\right)$$

$$D_y = \frac{E_r I_r}{l}\left[1 + \frac{\left(\bar{z}_r/\rho_r\right)^2}{1 + \frac{A_r}{lt}}\right]$$

$$E_x = E\left(\frac{A_s}{d} + t\right)$$

$$G_{xy} = Gt$$

$$E_y = E\left(\frac{A_r}{l} + t\right)$$

where ρ_s and ρ_r are the radii of gyration of a stringer and ring, respectively, about the centroid of the stiffener. As in the case of the corrugated cylinders, the dashed curve falls between curves associated with all internal and all external stiffening, but actually crosses the curve computed for

external stringers and internal rings. The agreement between the latter curve and that computed by using equation (16) is coincidental.

The dash-dot curves shown in figure 4 are general instability predictions based on a stability equation (eq. 7.7 of ref. 1) derived by Van der Neut. The differences between these curves and those of the present theory are attributed to the fact that, in Van der Neut's buckling theory, Poisson's ratio μ of the cylinder shell was taken to be zero everywhere except in computing the inplane shearing stiffness G_{xy} of the cylinder wall. Note, for example, in equation (17) that terms in $\mu\beta^2$ appear in the quantities Λ_r and Λ_{rs}, and hence that some differences might be expected between the present theory and one in which these terms were neglected. Moreover, computations using the present theory and Van der Neut's theory with Poisson's ratio set equal to zero everywhere in each of the two stability equations were found to be in excellent agreement for all three stiffening configurations shown in figure 4. It should be noted also that Van der Neut's equations were intended for use with stiffened cylinders having buckled skin and hence could be applied for this situation in lieu of equation (17). A modified form of equation (15) could also be used to analyze this type of stiffened cylinder; the orthotropic stiffnesses in this equation would be defined by effective width formulas which account for reduction in stiffness due to buckled cylinder skin.

Longitudinally Stiffened Cylinders

The susceptibility of the ring-and-stringer-stiffened cylinder configuration (fig. 2) to panel instability can be estimated by considering the cylinder wall between rings to be a compressed longitudinally stiffened cylinder that is simply supported at the rings. Panel instability predictions based on equation (18) are shown as the solid curves of figure 5 for stiffeners located on the internal or external surface of the cylinders.

The dashed curve shown in figure 5 is based on the stability equation of reference 11. The equation contained therein was derived from the Stein and Mayers equation (eq. (16)) and hence neglects eccentricity. Agreement between the dashed curve and the curve of the present theory for internally stiffened cylinders is believed to be merely coincidental. Also shown in figure 5 are curves computed from Van der Neut's stability equation (eq. 7.7 of ref. 1). The Van der Neut curve coincides with that of the present theory for internally stiffened cylinders and differs slightly only for short externally stiffened cylinders. The agreement suggests that the effect of Poisson's ratio in compressive buckling predictions of longitudinally stiffened cylinders may be small.

Attempts were also made to make panel instability predictions by using the buckling formula equation D-15 of reference 3. This formula was applied successfully to predict panel instability of several large-diameter integrally stiffened cylindrical panels and is appealing to designers because of its simplicity. Unfortunately, when applied to cylinders stiffened longitudinally by the Z-sections shown in figure 2, the formula gives different trends for internally and externally stiffened cylinders than those shown in figure 4. The

formula is believed to be in error by virtue of its bending stiffness term which forces longitudinal bending of the stiffened cylinder wall to occur about the middle surface of the cylinder skin. The agreement between the formula and the test data of the reference can be explained by observing that the neutral axis of the stiffener-shell composite considered in reference 3 occurs relatively near the middle surface of the skin. For many stiffened cylinder configurations, of course, bending does not occur in this fashion and therefore the formula has limited validity. Agreement was obtained between calculations based on the present theory and the test data of reference 3 for which the compressive buckling solution (eq. (18)) was appropriate.

Although the theoretical results contained herein are useful analytical tools, they do not necessarily encompass all the problems likely to face the designer of stiffened cylinders. References 3 and 4 have demonstrated the importance of boundary conditions as well as prebuckling deformations induced by eccentric loading in the analysis of longitudinally stiffened cylindrical shells. Reference 4 has also suggested that stiffened cylindrical shells may be stronger in bending than in compression and that discreteness of ring stiffeners can be signficant for certain stiffened shell configurations. The degree of importance of each of these effects will vary with the specific cylinder configuration under study, but nevertheless, the designer must be aware of their consequences.

CONCLUDING REMARKS

A small-deflection theory for buckling of stiffened orthotropic cylinders has been derived in a consistent manner by using the method of minimum potential energy. Equilibrium equations and admissible boundary conditions have been presented. Solutions to the governing equations which satisfy a set of boundary conditions comparable to that for simple support in classical shell buckling theory have been obtained for cylinders loaded with any combination of axial and circumferential loading.

The stability equations appropriate for stiffened orthotropic and isotropic cylinders have been presented and discussed. Differences between the solutions obtained for stiffened isotropic cylinders and the results of existing theories are noted; the differences in the equations of the existing theories stem from neglect of eccentricity, stiffness terms, or terms dependent on Poisson's ratio. Eccentricity effects in stiffened plates have also been discussed in an appendix.

Sample calculations have been shown for three types of stiffened cylinders to illustrate the importance of eccentricity effects in contemporary cylindrical structures loaded in compression. Substantial eccentricity effects are demonstrated in general instability predictions for ring-stiffened corrugated cylinders and ring-and-stringer-stiffened cylinders of proportions appropriate for large launch-vehicle interstage or intertank structures. Substantial effects are also shown in panel instability predictions for longitudinally stiffened

cylinders of similar proportions. Thus, account of eccentricity effects is shown to be imperative for accurate design calculations.

Langley Research Center,
National Aeronautics and Space Administration,
Langley Station, Hampton, Va., May 24, 1965.

APPENDIX A

BUCKLING OF STIFFENED PLATES

General Theory

Equilibrium equations for buckling of stiffened flat plates can be derived by following the procedure already outlined for stiffened cylinders. For plates, the midplane strain-displacement relations employed for the cylinder are replaced by

$$\epsilon_x = u_{,x}$$

$$\epsilon_y = v_{,y}$$

$$\gamma_{xy} = u_{,y} + v_{,x}$$

If this procedure is followed, equilibrium equations and boundary conditions identical to equations (11) and (13) with R taken to be infinitely large are obtained. Note that, unlike the usual flat-plate theory, equation (11c) does not become a simple equation in w alone, but that coupling terms remain as a result of eccentricity of the plate stiffeners. Thus, a one-sided effect is present in stiffened plates as well as cylinders.

Solutions for plates subjected to combinations of longitudinal and transverse loading $\overline{N}_x$ and $\overline{N}_y$ for simple-support boundary conditions can be obtained by assuming the following functions for displacements:

$$\left.\begin{aligned} u &= \bar{u} \cos \frac{m\pi x}{a} \sin \frac{n\pi y}{b} \\ v &= \bar{v} \sin \frac{m\pi x}{a} \cos \frac{n\pi y}{b} \\ w &= \bar{w} \sin \frac{m\pi x}{a} \sin \frac{n\pi y}{b} \end{aligned}\right\} \qquad \text{(A1)}$$

where a and b denote the stiffened plate length and width, respectively. The significance of solutions obtained for stiffened isotropic plates is discussed in the following paragraphs.

Solution for Buckling of Stiffened Isotropic Plates

The stability equation obtained by substituting the displacements specified in equations (A1) into the equilibrium equations for stiffened isotropic plates can be expressed as

$$\left(\bar{N}_x + \bar{N}_y\beta^2\right)\frac{a^2}{m^2\pi^2D} = \left(1 + \beta^2\right)^2 + \frac{E_sI_s}{dD} + \left(\frac{G_sJ_s}{dD} + \frac{G_rJ_r}{lD}\right)\beta^2 + \frac{E_rI_r}{lD}\beta^4$$

$$+ \frac{\frac{E_sA_s}{d}\bar{z}_s^2\left(1 + \beta^2\right)^2 + \frac{E_sA_s}{d}\frac{E_rA_r}{Etl}C_p + \frac{E_rA_r}{l}\bar{z}_r^2\beta^4\left(1 + \beta^2\right)^2}{D\left\{\left(1 + \beta^2\right)^2 + 2(1 + \mu)\beta^2\left(\frac{E_sA_s}{Etd} + \frac{E_rA_r}{Etl}\right) + \left(1 - \mu^2\right)\left[\frac{E_sA_s}{Etd} + 2(1 + \mu)\frac{E_sA_s}{Etd}\frac{E_rA_r}{Etl}\beta^2 + \frac{E_rA_r}{Etl}\beta^4\right]\right\}} \tag{A2}$$

where

$$C_p = \bar{z}_s^2\beta^2\left[2(1 + \mu) + \left(1 - \mu^2\right)\beta^2\right] + 2\bar{z}_s\bar{z}_r(1 + \mu)^2\beta^4$$

$$+ \bar{z}_r^2\beta^4\left[1 - \mu^2 + 2\beta^2(1 + \mu)\right]$$

and

$$\beta = \frac{na}{mb}$$

In equation (A2), the subscript s now denotes longitudinal stiffening (parallel to the x-axis) and the subscript r now denotes transverse stiffening (parallel to the y-axis).

Equation (A2) is appropriate for buckling of simply supported isotropic plates stiffened longitudinally and transversely with sturdy stiffeners. Buckling is assumed to occur with long sinusoidal waves encompassing several stiffeners. Note in equation (A2) that if the plate is stiffened by only longitudinal or transverse stiffeners, all terms involving $\bar{z}_s$ or $\bar{z}_r$ are squared and hence the surface on which the stiffener is located is unimportant (as might be expected intuitively). However, if both longitudinal and transverse stiffening are present, the coupling term C_p in equation (A2) has terms with the coefficient $\bar{z}_r\bar{z}_s$ which can change sign if the longitudinal and transverse stiffeners are on opposite sides of the plate.

If the plate is stiffened longitudinally and loaded in compression, equation (A2) can be written as

$$\frac{\bar{N}_xa^2}{m^2\pi^2D} = \left(1 + \beta^2\right)^2 + \frac{G_sJ_s}{dD}\beta^2 + \frac{(EI)_{eff}}{dD} \tag{A3}$$

where

$$(EI)_{eff} = E_s I_s + \frac{E_s A_s \bar{z}_s^2}{1 + Z_{mn} \frac{E_s}{E} \frac{A_s}{td}}$$

with the coefficient Z_{mn} defined by

$$Z_{mn} = \frac{2\beta^2(1 + \mu) + 1 - \mu^2}{\left(1 + \beta^2\right)^2}$$

When the twisting stiffness $G_s J_s$ is taken to be zero, equation (A3) with $n = 1$ can be shown to be identical in form to the stability equation obtained by Seide and Stein (eq. (1) of ref. 12) if, in the reference, the product of number of bays and the stiffener spacing is replaced by the plate width b.

In equation (A3), $(EI)_{eff}$ is the effective bending stiffness of the stiffener-plate combination. Note that $(EI)_{eff}$ is a function of the buckle aspect ratio parameter β and the eccentricity $\bar{z}_s$. An analysis of the effective bending stiffness for plates with one, two, or three stiffeners was made by Seide in reference 13. Although the results of the present theory are based on investigation of sinusoidal buckling modes, which encompass several stiffeners and hence cannot be compared directly with the results of reference 13, both analyses give the result that bending of plate columns ($a/b = 0$) occurs about the neutral axis of the plate-stiffener combination $\left(\text{i.e., } Z_{mn} = 1 - \mu^2\right)$.

REFERENCES

1. Van der Neut, A.: The General Instability of Stiffened Cylindrical Shells Under Axial Compression. Rept. S. 314, Natl. Aeron. Res. Inst. (Amsterdam), 1947.

2. Baruch, M.; and Singer, J.: Effect of Eccentricity of Stiffeners on the General Instability of Stiffened Cylindrical Shells Under Hydrostatic Pressure. J. Mech. Eng. Sci., vol. 5, no. 1, 1963, pp. 23-27.

3. Anon.: Theoretical and Experimental Analysis of Orthotropic-Shell Stability. LMSC-A701014, Lockheed Missiles & Space Co., Sept. 11, 1964.

4. Hedgepeth, John M.; and Hall, David B.: Stability of Stiffened Cylinders. Paper No. 65-79. Am. Inst. Aeron. Astronaut., Jan. 1965.

5. Card, Michael F.: Preliminary Results of Compression Tests on Cylinders With Eccentric Longitudinal Stiffeners. NASA TM X-1004, 1964.

6. Mechtly, E. A.: The International System of Units - Physical Constants and Conversion Factors. NASA SP-7012, 1964.

7. Stein, Manuel; and Mayers, J.: A Small-Deflection Theory for Curved Sandwich Plates. NACA Rept. 1008, 1951. (Supersedes NACA TN 2017.)

8. Budiansky, Bernard; and Seide, Paul: Compressive Buckling of Simply Supported Plates With Transverse Stiffeners. NACA TN 1557, 1948.

9. Marguerre, Karl: On the Application of the Energy Method to Stability Problems. NACA TM 1138, 1947.

10. Stein, Manuel; and Mayers, J.: Compressive Buckling of Simply Supported Curved Plates and Cylinders of Sandwich Construction. NACA TN 2601, 1952.

11. Peterson, James P.; and Dow, Marvin B.: Compression Tests on Circular Cylinders Stiffened Longitudinally by Closely Spaced Z-Section Stringers. NASA MEMO 2-12-59L, 1959.

12. Seide, Paul; and Stein, Manuel: Compressive Buckling of Simply Supported Plates With Longitudinal Stiffeners. NACA TN 1825, 1949.

13. Seide, Paul: The Effect of Longitudinal Stiffeners Located on One Side of a Plate on the Compressive Buckling Stress of the Plate-Stiffener Combination. NACA TN 2873, 1953.

TABLE I.- BUCKLING PREDICTIONS FOR STIFFENED CYLINDERS

(a) Ring-stiffened corrugated cylinders

$\frac{l}{R}$	$\frac{\bar{N}_x}{E_x}$	m	n
Rings - external			
0.15	0.005061	2	0
.20	.004289	2	0
.25	.003826	2	0
.30	.003517	2	0
.35	.003297	2	0
.40	.003132	2	0
.45	.003003	2	0
.50	.002900	2	0
Rings - internal			
0.15	0.001761	1	6
.20	.001491	1	6
.25	.001324	1	6
.30	.001210	1	6
.35	.001126	1	6
.40	.001061	1	6
.45	.001009	1	6
.50	.000967	1	6

(b) Ring-and-stringer-stiffened cylinders

$\frac{l}{R}$	$\frac{\bar{N}_x}{E\bar{t}}$	m	n
Stringers - external; rings - external			
0.05	0.005970	3	6
.10	.005121	3	6
.15	.004733	3	7
.20	.004467	3	7
.25	.004137	3	8
Stringers - external; rings - internal			
0.05	0.004111	3	7
.10	.003836	3	7
.15	.003720	3	8
.20	.003629	3	8
.25	.003574	3	8
Stringers - internal; rings - internal			
0.05	0.003764	3	7
.10	.003430	3	7
.15	.003160	2	7
.20	.002988	2	7
.25	.002779	2	8

(c) Longitudinally stiffened cylinders

$\frac{l}{R}$	$\frac{\bar{N}_x}{E\bar{t}}$	m	n
Stiffeners - external			
0.15	0.007043	1	0
.20	.004739	1	8
.25	.003614	1	18
.30	.002814	1	25
.35	.002243	1	27
.40	.001843	1	27
.45	.001554	1	26
.50	.001340	1	25
Stiffeners - internal			
0.15	0.006747	1	21
.20	.003804	1	20
.25	.002443	1	19
.30	.001706	1	18
.35	.001262	1	18
.40	.000975	1	18
.45	.000780	1	18
.50	.000641	1	17

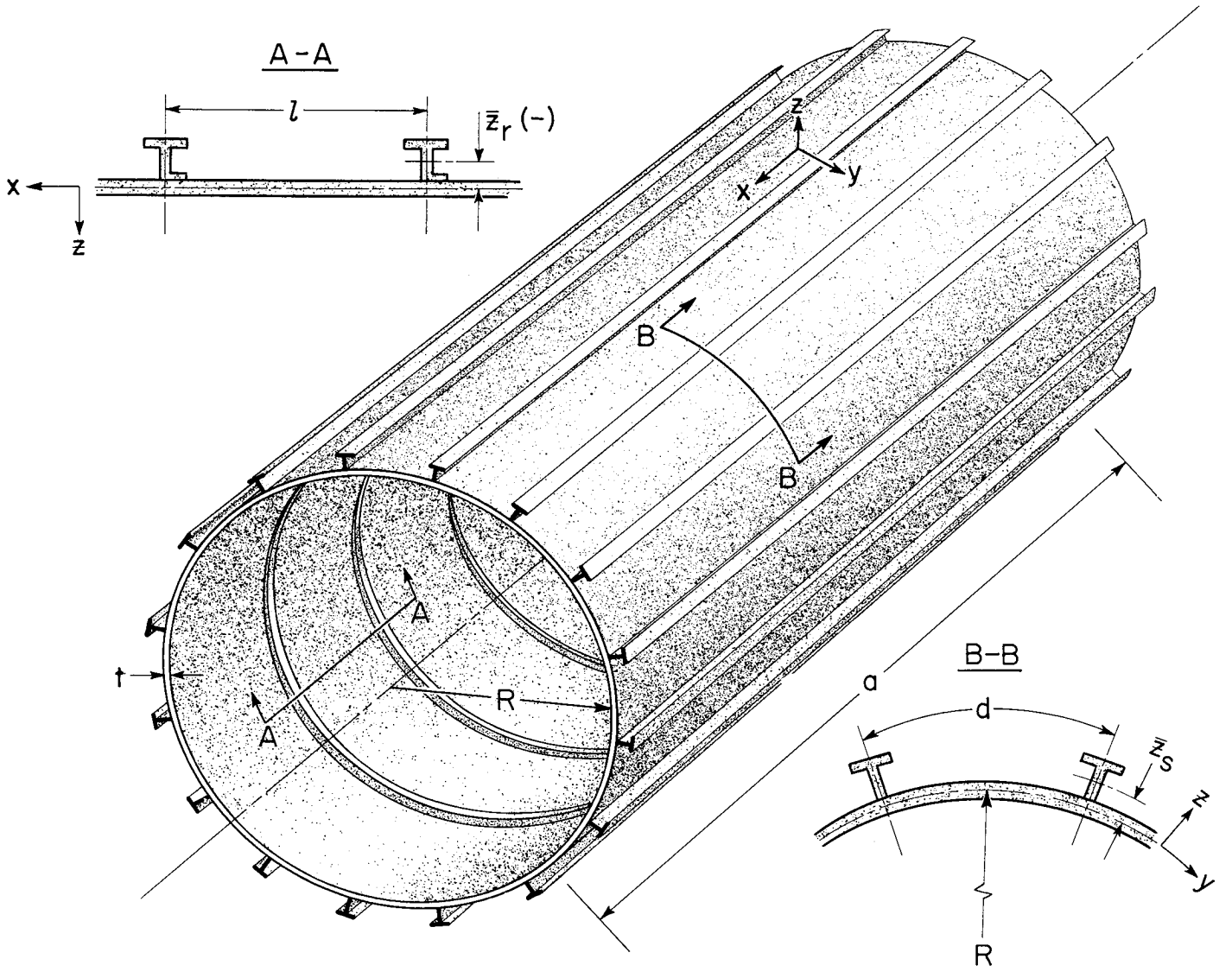

Figure 1.- Geometry of stiffened cylinder.

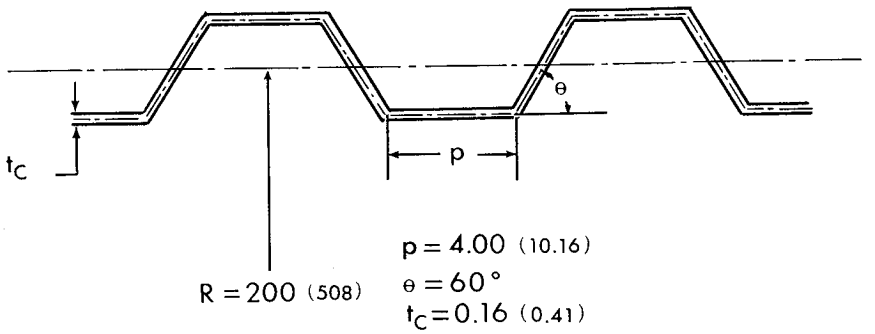

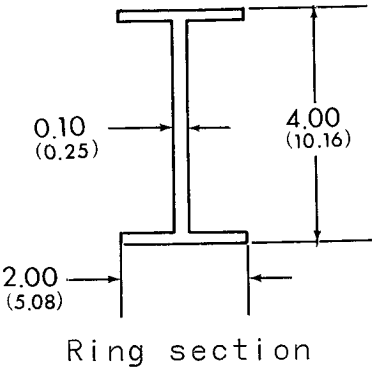

(a) Ring-stiffened corrugated cylinders; a = 200 in. (508 cm).

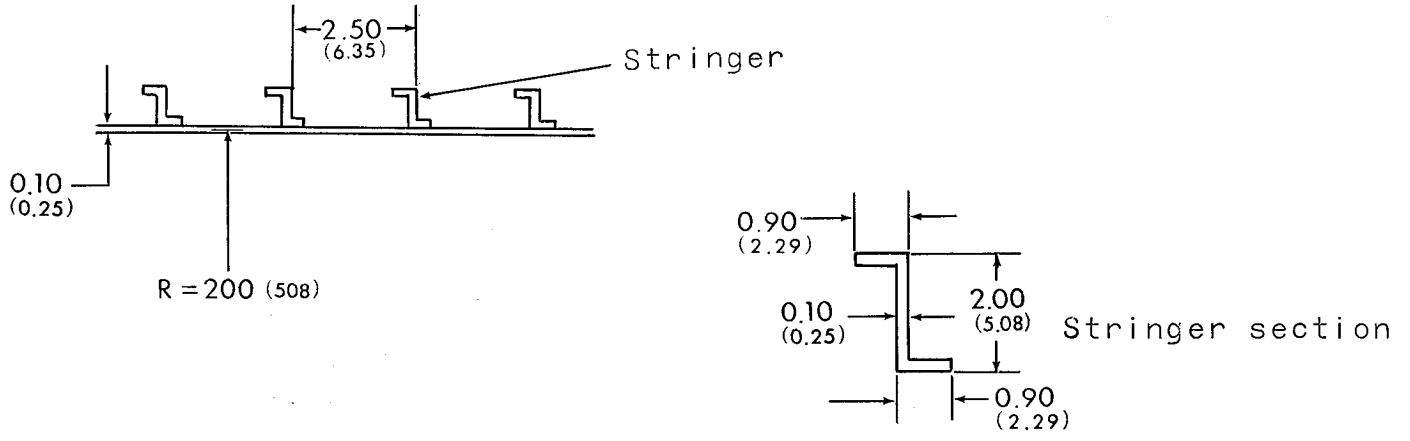

(b) Ring-and-stringer-stiffened cylinders; a = 200 in. (508 cm). (See fig. 2(a) for ring section.)

Figure 2.- Dimensions of stiffened cylinder walls. Dimensions are in inches. (Parenthetical dimensions in cm.)

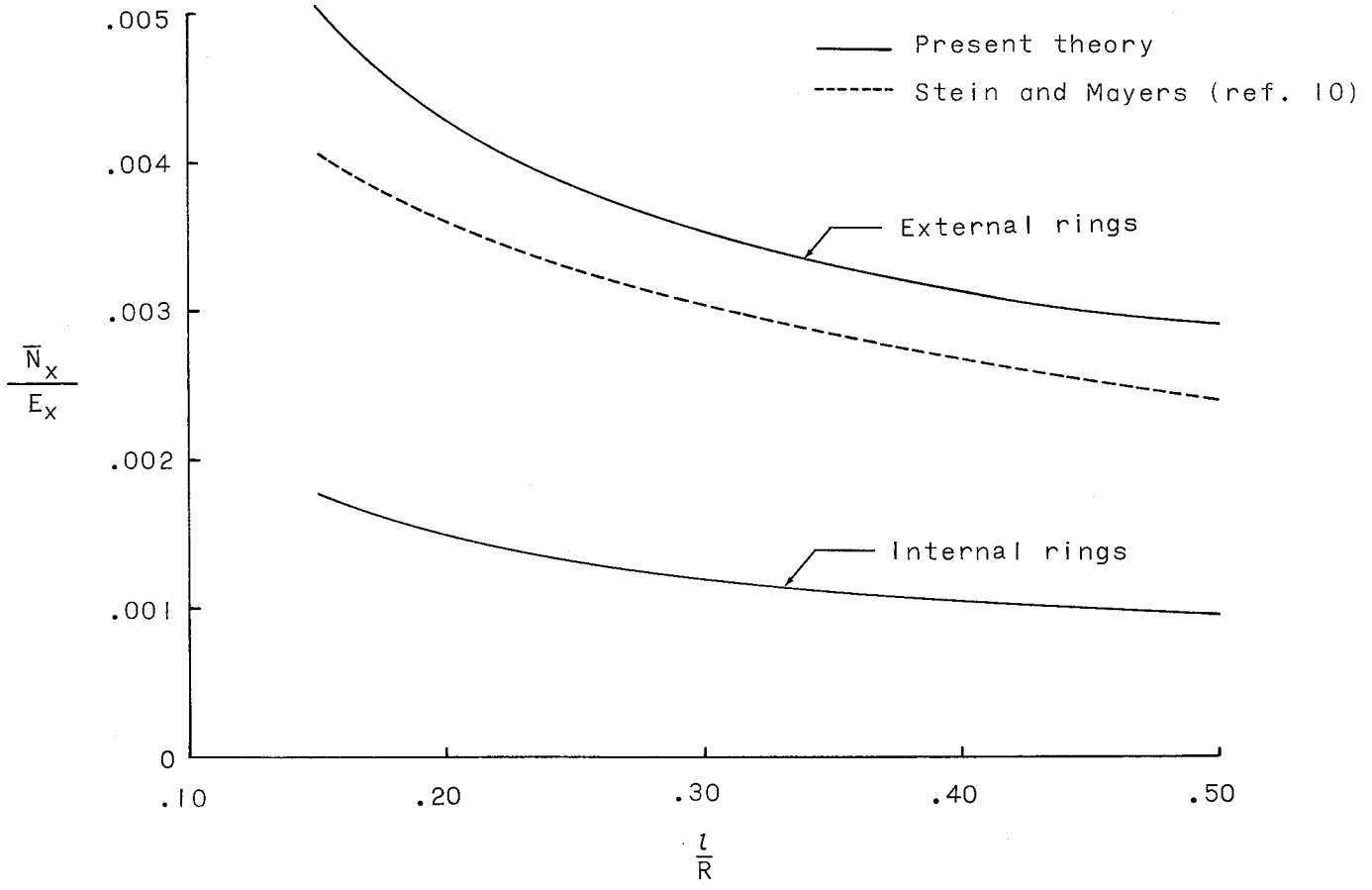

Figure 3.- General instability predictions for compressed ring-stiffened corrugated cylinders.

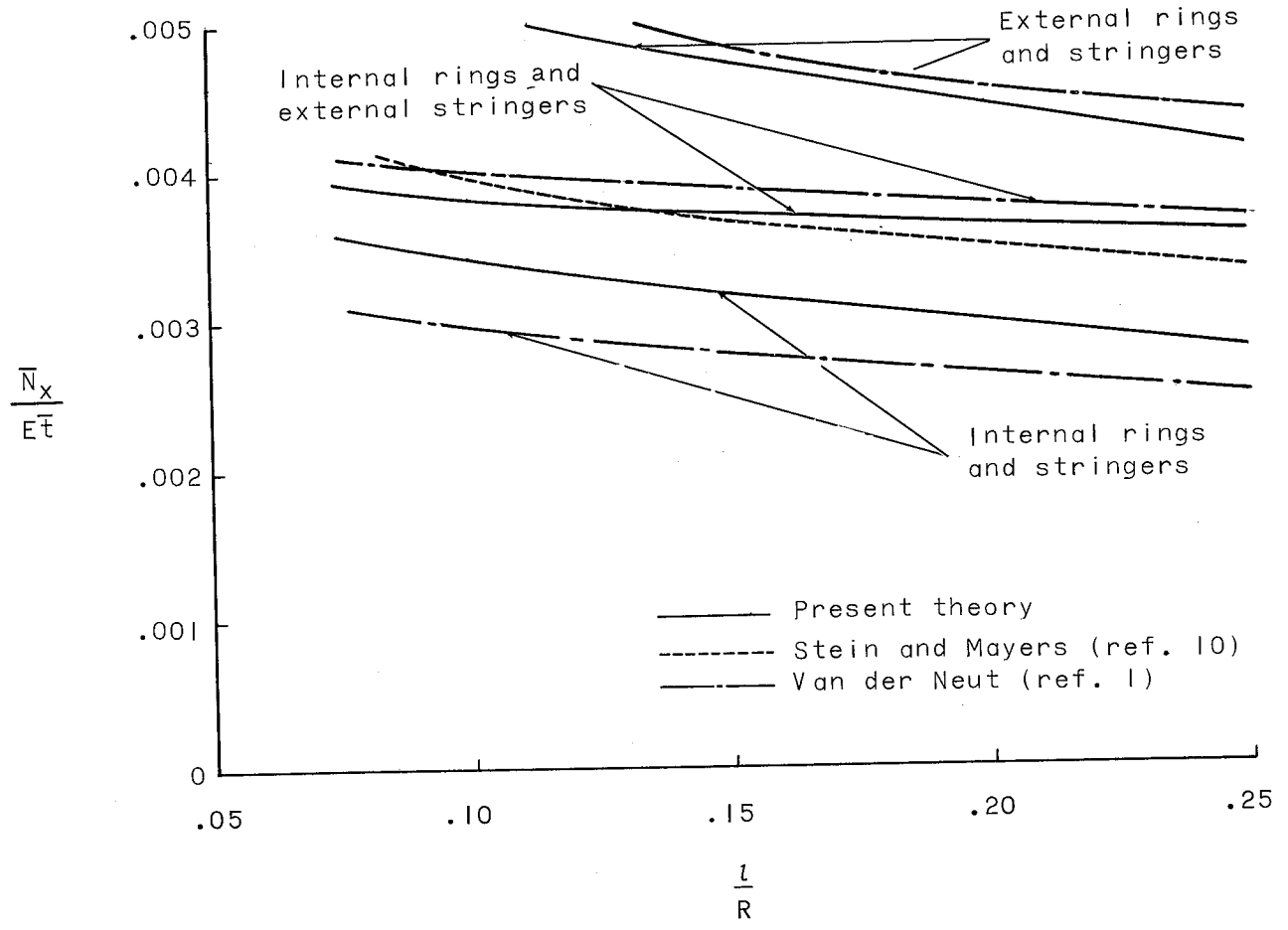

Figure 4.- General instability predictions for compressed ring-and-stringer-stiffened cylinders.

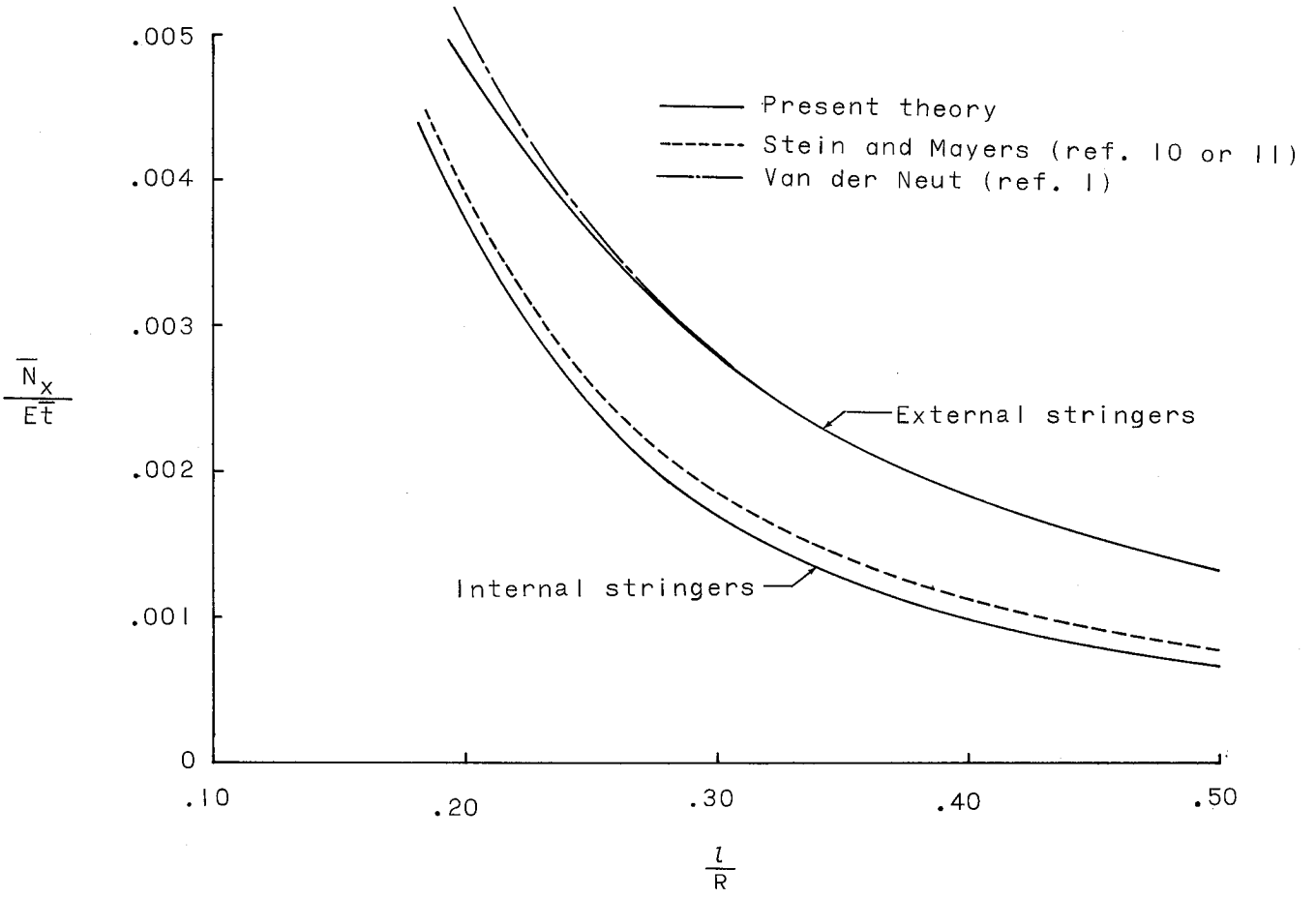

Figure 5.- Panel instability predictions for compressed longitudinally stiffened cylinders.